Hindawi
Geofluids
Volume 2022, Article ID 3141964, 13 pages
https://doi.org/10.1155/2022/3141964

Research Article

Impact of Isothermal Layering on the Stability of Saline Soil Subgrade in Cold Regions

Yu Zhang,[1] **Xuerui Chen**,[2] **Meisi Zou**,[3] **Runze Tian**,[1] **Yunlong Hou**,[4] **and Bingbing Han**[4]

[1]*School of Traffic and Transportation, Lanzhou Jiaotong University, Lanzhou 730070, China*
[2]*Lanzhou Rail Transit Construction Management Office, Lanzhou 730070, China*
[3]*School of Automotive Engineering, Jiujiang Vocational and Technical College, Jiangxi 332000, China*
[4]*Gansu Institute of Engineering Geology, Lanzhou 730000, China*

Correspondence should be addressed to Yu Zhang; zhangyu@mail.lzjtu.cn

Received 18 December 2021; Accepted 7 March 2022; Published 4 April 2022

Academic Editor: Qingzhi Wang

In order to determine the influence of heat on the stability of the saline soil subgrade slope in cold regions. Firstly, four typical representative saline soils were selected as subgrade fillers, and geotextiles were added at the bottom of the subgrade as a study subject. A two-dimensional numerical model for the temperature field of subgrade soil was established based on COMSOL Multiphysics. Secondly, combined with the main strength parameters of subgrade soil at different temperatures, an isothermal stratification-strength parameter function calculation model was proposed. Then, the SLOPE/W module in GeoStudio is used to stratify the established subgrade model according to isotherms and calculate the stability safety factor of saline soil subgrades in cold regions under different months, slopes, and subgrade heights, respectively. Finally, the influence of submergence at the foot of the slope on the stability of the subgrade slope is discussed. The results show: After the cold season coming, with the decreasing of temperature, the stability of HC-1 and HC-2 saline soil subgrade slope increased to different extents when the ground temperature dropped to -10°C. When the local temperature dropped below -10°C, the stability has slight decline; CS-1 and CS-2 saline soil subgrade in the ground temperature dropped to 10°C (HC-1 and HC-2 denote two groups of saline soil with high chloride-salt content (≥15%) and low sulfate salt content (≤0.5%), whereas CS-1 and CS-2 denote two groups of saline soil with low chloride-salt (≤5%)), the slope stability was significantly improved, and the stability of CS-1 increases slightly with further decrease in temperature.

1. Introduction

Highway distress in China, such as salt swelling, muddying, wet (solution) subsidence, and corrosion, occurs frequently in saline soil areas, which seriously affects the performance of subgrade [1]. Research from McRobert and Foley [2] showed that soil at areas of high salinity and high groundwater levels could produce salt crystals with the change of external temperature. The result could be the destruction of the internal structure of the soil, which will inevitably lead to the decline of the overall strength and stability of the subgrade.

In cold regions, different kinds of salt in saline soil could produce corresponding salt crystals or mirabilite at different ambient temperatures, which will change the volume and strength of the soil. Therefore, the internal structure of the soil will be changed accordingly and the strength of the soil will be destroyed. Swenne [3] pointed out that salt will crystallize and $NaCl \bullet 2H_2O$ will form out of the chloride-salt and unfrozen water when the temperature is lower than 0°C. Liao and Archer [4, 5] mentioned that $Na_2SO_4 \bullet 10H_2O$ will be produced out of sulfate and unfrozen water when the temperature reaches 33° C. Different kinds of salt in the soil affects its freezing temperature. Bing and Ma [6] found that the freezing temperature will drop when salinity increases, and the temperature rises when water content increases. The freezing temperature of the soil varies in accordance with the type of salt contained. The effects of common anions in the soil on freezing temperature can be listed as Cl^-, CO_3^{2-}, and SO_4^{2-}. The influence of common cations in

the soil on the freezing temperature can be ranked in descending order of magnitude as K^+, Na^+, and Ca^{2+}. Banin and Anderson [7] proposed an equation to calculate the freezing temperature through the soluble salt content in porous medium. Predecessors explored the relationship between different temperature and different salinity crystallization. However, the different salt crystals generated by the high salt content saline soil in the cold season under non-freezing conditions directly affect the soil strength. Therefore, it is meaningful to discuss the effects of temperature and soil strength parameters on the stability of saline soil subgrade.

Stability theories of subgrade slopes in cold region have previously been done. Weeks [8] deduced the "ice blocking seepage" model, in which they discovered that the excess pore water pressure was formed, for the lower layer of molten soil prevented the outward discharge of pore water. Another research done by Hutchinson [9] used the total stress analysis method. He found that the reduction of undrained shear strength of soil, which was caused by the increase of the water content when the soil melted, could trigger the instability of the slope. In addition, the increase of water content could also cause the accumulation of fragment ice on the frozen frontal surface. McRoberts and Morgenstern [10] pointed out that the melting or consolidation process of frozen soil on slopes increases the super-pore water pressure inside the soil, which eventually leads to slope instability. Although research on the mechanism of slope instability has been done, reports on the slope stability of saline soil subgrade and the change of the strength of the soil at its different depths caused by the temperature field change are seldom seen.

In summary, the value of soil strength in most of the studies on slope stability of road base usually takes soil type into consideration only, instead of combining the climate condition at the construction site and soil characteristics in cold region, because under the effect of heat, the change amplitude of soil strength parameter is large, which will cause the change of slope stability of road base. Due to the large variation amplitude of soil strength parameters under thermal action, the stability of subgrade slope changes. Therefore, it is particularly important to study the stability of saline soil subgrade slope with different salinity and different salt types under thermal action.

2. Project Background

The highway from Qarham to Golmud, which is located at the area where its altitude varies greatly, crosses subtropical and cold temperate zones. It is dry here and lack of rainfall with large annual evaporation. The place has four distinctive seasons. The temperature can be as low as -33°C in cold season and reaches 35°C in warm season. The temperature difference between day and night is great [10–12].

According to the actual engineering geology, a meteorological station was established at K664+360 of the Qarham-Golmud highway to monitor the weather conditions and the surface and underground temperature in Qarham, where temperature probes were placed at the surface, 40 cm underground, 80 cm underground, 160 cm underground, and 320cm underground, respectively, and collected once or twice a day. Finally, the data were aggregated to obtain the temperature and ground temperature changes in different months of the year.

As Figure 1 shows, the monthly average temperature of this region in July was the highest, reaching 23°C. The monthly average temperature in June, July, and August was above 15°C; the lowest temperature in December was as low as -9.2°C; 11, 12, 1, 2,. The monthly average temperature in November, December, January, February, and March was below 0°C. The temperature difference between the highest temperature and the lowest temperature was 32.2°C. The temperature changes significantly in four seasons, and conforms to the law of sinusoidal function in general. The temperature difference between day and night in winter and summer is large. The land surface temperature is close to the air temperature here. There is a significant difference between the ground temperature at 40 cm below the surface and the air temperature. The deeper the depth, the greater the temperature difference. The ground temperature at 320 cm below the surface is quite different from the air temperature. The ground temperature generally conforms to the trend of a sinusoidal function. The deeper the depth, the smaller the temperature change, and the ground temperature changes slightly around 10°C at 320 cm below the surface.

The Qarham-Golmud highway passes Qarham Salt Lake, Garsu Station, Yushui River, with a total length of 80.052 kilometers. The expressway was constructed with bi-directional and four-lane. The design speed is 100 kilometers per hour, the subgrade is 26 meters wide, and the pavement structure is bituminous concrete. The saline soil along the highway covers a large area, whose salt composition and content have regional differences [13]. The high salinity soil sampling points along the Qarham-Golmud highway are shown in Figure 2.

The temperature in the cold and warm seasons in this area is quite different, and the saline soils in the test section of soluble salts are mainly chloride-saline soils, whose physical and mechanical properties are susceptible to temperature changes. In this case, a large amount of salt crystals are generated at the foot of the slope and the drainage ditch, which will change the internal structure of the soil, its strength could be reduced, and the stability of the subgrade slope will change accordingly. According to the chemical analysis of soluble salts towards salinity of the soil along the high by Zhang et al. [14], the soil along the Qarham-Golmud highway was mainly chloride-salinized soil with a small amount of sulfate salty soil. The salinity is mainly between 3% and 50%. Most of the soils here belong to over-salted soil and strong saline soil. According to the freezing temperature test of some saline soils in this area by Zhang et al. [15], three types of saline soils (HC-1, HC-2, and CS-1) selected from the article will not freeze at -20° C, so they will not freeze under the ground temperature in the cold season in this area.

3. Computational Model

COMSOL Multiphysics is based on the finite element method, which can be used to describe the temperature and moisture fields of saline soil subgrade using two partial differential equations [16].

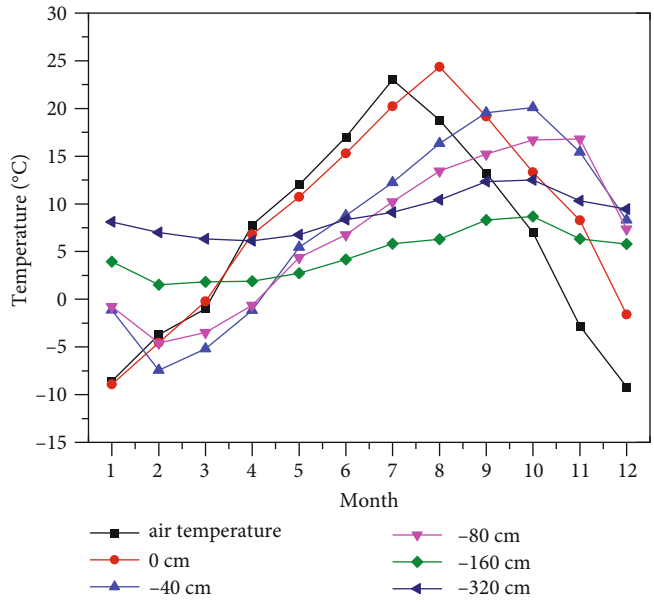

Figure 1: Average temperature and ground temperature from 2016 to 2020.

(a) Visible salt crystals (white) (b) Drainage along the highway

Figure 2: High salinity soil sampling points along Qarham-Golmud highway.

3.1. Temperature Field Governing Equation. According to the basic theory of heat transfer, using the latent heat of phase transition as the internal heat source, the differential equation of heat conduction can be expressed by equation (1):

$$\rho C(\theta)\frac{\partial T}{\partial t} = \nabla \cdot (\lambda(\theta)\nabla T) + \mathrm{L_I} \cdot \rho_\mathrm{I}\frac{\partial \theta_I}{\partial t} + \mathrm{L_c} \cdot \rho_\mathrm{c}\frac{\partial \theta_c}{\partial t}. \quad (1)$$

In the equation, the latent heat of phase change is used as the heat source, and the latent heat of ice is extended to the latent heat of ice and salt crystals. Salt crystals only consider salt crystals ($NaCl \cdot 2H_2O$) and mirabilite ($NaSO_4 \cdot 10H_2O$). ρ, ρ_I, and ρ_c are the density of the soil, the density of ice, and the density of salt crystals(kg/m^3);

$C(\theta)$ is the specific heat (J/(kg·°C)); T is the transient temperature of the soil; t is the time (s); $\lambda(\theta)$ is the thermal conductivity of the soil (W/(m·°C)); ∇ is the Hamiltonian; L_I is the latent heat of phase transition of water; L_c is the latent heat of phase transition of salt; θ, θ_I, and θ_c are the volumetric water content, the pore ice volume content, and the salt crystal volume content. For parameter values, refer to reference [17].

3.2. Governing Equation of Water Field. The movement of unfrozen water in the subgrade soil follows Darcy's law. Water migration in unsaturated soils can be represented by Richard's equation [14] using equation (2):

$$\frac{\partial \theta_u}{\partial t} + \frac{\rho_I}{\rho_\mathrm{w}} \cdot \frac{\partial \theta_I}{\partial t} = \nabla \cdot \left[D(\theta_u)\nabla\theta_u + k_g(\theta_u)\right]. \quad (2)$$

In the equation, $\partial\theta_u/\partial t$ represents the change of unfrozen water content with time, $\rho_I \cdot \partial\theta_I/\partial t$ represents the change of ice content with time, and $\nabla\cdot[D(\theta_u)\nabla\theta_u + k_g(\theta_u)]$ represents the migration of water. k_g is the permeability coefficient of unsaturated soil in the direction of gravity acceleration; $D(\theta_u)$ is the diffusivity of unfrozen water in frozen soil [18]. The calculation equation is shown in equation (3):

$$D(\theta_u) = \frac{k(\theta_u)}{c(\theta_u)} \cdot I. \quad (3)$$

Among them, $k(\theta_u)$ is the permeability (m/s) of the unsaturated soil; $c(\theta_u)$ is the specific water capacity (1/m); I is the

impedance factor, which indicates that the pore ice blocks the unfrozen water migration, $I = 10^{10\theta_I}$.

3.3. Simultaneous Equations. Based on experimental data, Xu [19] gave an empirical expression for the unfrozen water content in frozen soil, as shown in equation (4):

$$\frac{w_0}{w_u} = \left(\frac{T}{T_f}\right)^B, T < T_f. \tag{4}$$

In the equation, w_0 is the initial moisture content of the soil (%); w_u is the moisture content of the unfrozen water (%) when the negative temperature is T; T_f is the freezing temperature of the soil (°C), which can be determined through experiments. According to the physical characteristics analysis of the soil sample, the soil sample is silty clay, B is a constant, approximately 0.56.

The "solid-liquid ratio" [20] represents the ratio of the volume of pore ice to unfrozen water in frozen soil, and is written as. According to equation (5), there are:

$$B_I = \frac{\theta_I}{\theta_u} = \begin{cases} 1.1\left(\dfrac{T}{T_f}\right)^B - 1.1 & \left(T < T_f\right) \\ 0 & \left(T \geq T_f\right) \end{cases}. \tag{5}$$

In the equation, the coefficient 1.1 is the ratio of the density of water to ice.

From equation (5), we know that the solid-liquid ratio B_I is a single value function of temperature. Therefore, the relational equation of pore ice, unfrozen water, and temperature in frozen soil can be expressed by equation (6) as:

$$\theta_I = B_I(T) \cdot \theta_u \tag{6}$$

3.4. Calculation Parameters and Boundary Conditions

3.4.1. Thermal Characteristics of Soil. The thermal properties of soil mainly include thermal conductivity and volume-specific heat capacity. By consulting the literature [20, 21], the specific values are shown in Table 1.

3.4.2. Boundary Conditions. The boundary conditions of the subgrade temperature field include the first type of boundary conditions, the second type of boundary conditions, and the third type of boundary conditions. In the subgrade temperature field hydrothermal coupling model, the first type of boundary conditions is adopted for the pavement, shady slope, and sun slope, and the second boundary condition of constant geothermal flow is adopted for the lower boundary. The thermal boundary condition at the bottom is taken as the temperature gradient, 0.03°C/m [22–24].

The first type of boundary conditions [14] used on pavements, shades, and sun slopes can be fitted by equation (11):

$$T = T_0 + G(t) + A \sin(\omega t + \varphi) \tag{7}$$

Table 1: Soil thermal parameters.

Name	λ_f/(W·m^{-1}·°C^{-1})	λ_u/(W·m^{-1}·°C^{-1})	C_f/(J·m^{-3}·°C^{-1})	C_u/(J·m^{-3}·°C^{-1})	L_c/(J·m^{-3})
Silty clay	1.351	1.125	2.357×10^6	1.879×10^6	60.3×10^6

In the equation, T_0 on the right side of the equation represents the average temperature, and A represents the amplitude, which is the maximum temperature fluctuation in a cycle. The road, shady slope, and sun slope correspond to different amplitudes. ω is to determine the period of temperature change, generally 365×24 h, and here the unit is calculated in seconds, $365 \times 24 \times 3600$s. φ usually the physical meaning in the sine function is the primary phase, and the value is generally determined according to the moment of starting the simulation. $G(t)$ is a function of time that increases the temperature of the Tibetan Plateau over the next 50 years by 2.2~2.6° C [25, 26]. The maximum temperature rise in this model in the next 50 years is 2.6° C, and its expression can be expressed by equation (12):

$$G(t) = C \times t. \tag{8}$$

In the equation, C is $0.052/8760 \times 3600$ on the right side of the equation, and t represents time in seconds.

According to the attached surface theory [15], the least square method is used for fitting, and the values of T_0, A, and φ are obtained, as shown in equations (13) to (16).

$$\text{Road surface}: T(t) = 10.71 + 16.9 \sin\left(\frac{2\pi}{365 \times 24 \times 3600} t + 1.43\right) + \frac{0.052t}{365 \times 24 \times 3600} \tag{9}$$

$$\text{Sun slope}: T(t) = 8.85 + 16.32 \sin\left(\frac{2\pi}{365 \times 24 \times 3600} t + 1.41\right) + \frac{0.052t}{365 \times 24 \times 3600} \tag{10}$$

$$\text{Shady slope}: T(t) = 7.65 + 16.04 \sin\left(\frac{2\pi}{365 \times 24 \times 3600} t + 1.42\right) + \frac{0.052t}{365 \times 24 \times 3600} \tag{11}$$

$$\text{Natural surface}: T(t) = 8.6 + 15.89 \sin\left(\frac{2\pi}{365 \times 24 \times 3600} t + 1.42\right) + \frac{0.052t}{365 \times 24 \times 3600} \tag{12}$$

3.5. Geometric Model. The subjects of the study are subgrade and partial foundation. Combined with the actual engineering situation of the Qarham-Golmud highway test section, a two-dimensional axisymmetric subgrade model is established, with

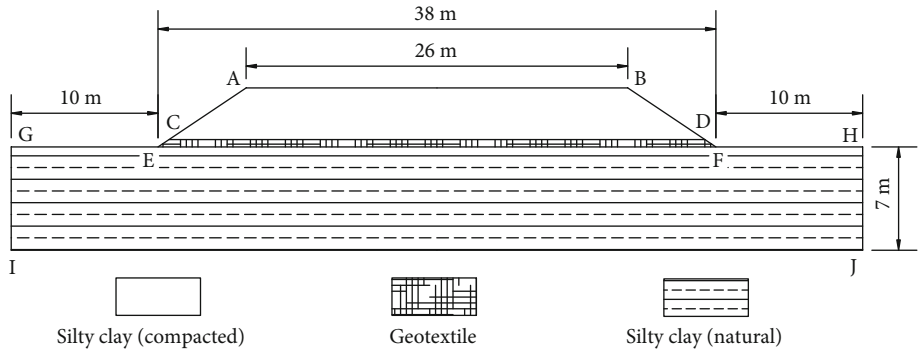

Figure 3: Subgrade schematic.

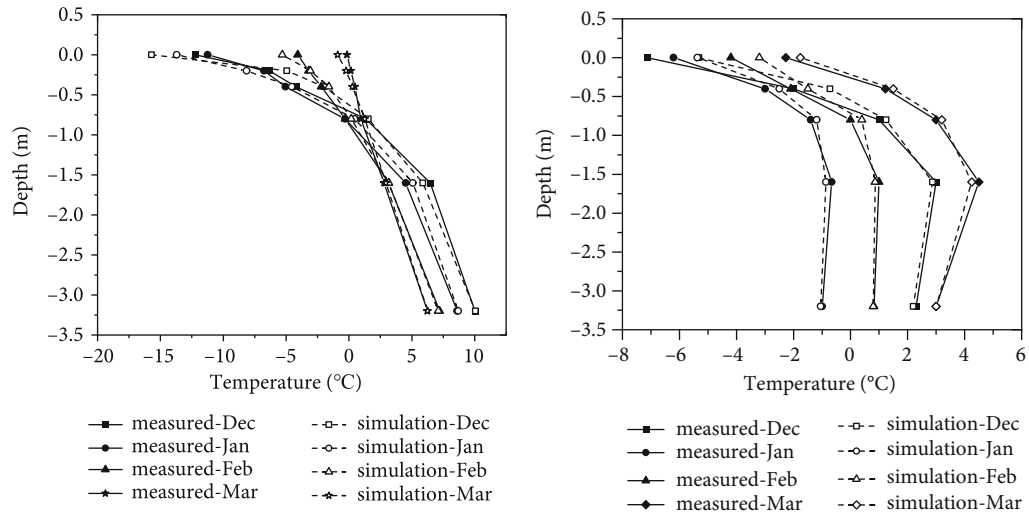

Figure 4: High salinity soil sampling points along Qarham-Golmud highway.

a road width of 26 m, a subgrade height of 4 m, and a slope of 1 : 1.5. The bottom of the subgrade is paved with geotextiles at a distance of 0.5 meters on the ground.

Subgrade filling is compacted silty clay, and the foundation soil is silty clay (Figure 3).

3.6. Validation of Ground Temperature Simulation. Due to the low water content of the subgrade soil with scarce precipitation in the area, the groundwater source was blocked by the addition of geotextiles to the subgrade. Therefore, the problem of salt and water migration due to temperature gradients was not considered.

Comparing the theoretical calculation results of the ground temperature below the natural ground and at the mid-line of the subgrade with the actual ground-bore ground temperature test data in the cold season (Figure 4), it can be seen that:

(a) Natural ground surface

(b) Subgrade central line

(1) The simulation results of soil temperature at different depths are consistent with the field measurement results. In the shallow layer, the simulation result and the actual measurement are quite different; in the deep layer, the difference between the simulation result and the actual measurement is small. The main reason is that the external environment changes greatly, and the surface layer is greatly affected by the accumulation effect of the external environment. As the depth increases, this effect gradually decreases

(2) The measured results of the subgrade temperature in the four months of the cold season (December, January, February, and March) are in good agreement with the simulation results. From the subgrade depth of 0 cm to the subgrade depth of 60 cm, the measured values are different from the simulation results, but the differences are not significant. When the depth reaches 160 cm to 320 cm, the measured value is very close to the simulation result

(3) On the whole, the numerical simulation results are very close to the measured data of boreholes. The change trends are consistent, which verifies the validity of the model

Table 2: Saline soil properties parameter table.

Sampling position	Soil sample	Proportion	Liquid limit (%)	Plastic limit (%)	Soil sample category	Optimal moisture content (%)	Maximum dry density (g/cm^3)	Saturation (%)
K603+260	HC-1	2.42	26.3	17.4	Low-plasticity clay	6.6	1.96	75.6
K602+750	HC-2	2.58	28.5	18.2	Low-plasticity clay	8.7	1.83	58.6
K636+000	CS-1	2.65	38.7	25.4	Low-plasticity clay	16.9	1.77	95.5
K642+200	CS-2	2.55	42.0	27.3	Silt	17.8	1.66	89.5

Table 3: Saline soil salt content.

Soil sample	Content of selected salts (weight %)							Total salt content (%)
	CO_3^{2-}	HCO_3^-	Cl^-	SO_4^{2-}	Ca^{2+}	Mg^{2+}	Total	
HC-1	0.03	0.13	17.93	0.48	0.60	0.98	20.14	36.1
HC-2	0.00	0.03	14.73	0.24	0.60	1.34	16.95	25.4
CS-1	0.00	0.01	3.37	1.49	0.70	0.24	5.81	11.9
CS-2	0.00	0.16	0.53	0.72	0.30	0.24	1.96	2.6

4. Test and Value of Strength Parameters of Subgrade Soil

4.1. Physical and Chemical Test Parameters. In order to study the situation of saline soil along the line comprehensively and accurately, and to investigate and analyze the distribution of saline soil along the way, four soil samples with different salinity were selected at the following four mileage piles. Results from test by Zhang et al. [14] about physical properties are as shown in Table 2 and its salinity are as shown in Table 3. In the table, HC-1 and HC-2 represent samples of high-chlorine saline soils, and CS-1 and CS-2 represent samples of relatively high-sulfate chloride-saline soils.

4.2. Freezing Temperature Experiment. The freezing temperature of the soil is affected by salinity. CS-1 and CS-2 soil samples with low total salt content were selected for the freezing temperature experiment. At the beginning of the experiment, a starting temperature was preset in order to reduce the data collection effort while achieving the experimental purpose. After the temperature was reached, the configured soil samples were successively put into the prepared bags, inserted into the temperature collection probes, sealed, and put into the cold liquid of the low-temperature thermostat. Then, the low-temperature thermostat was adjusted again, and the preset temperature was set to -10°C and -20°C, respectively. The computer was started, the software was opened, and the temperature collection interval was set to 10s, so that the temperature changes inside the sample could be collected on the computer. When the display temperature of the low-temperature thermostat reaches -10°C and -20°C, the acquisition is stopped and the instrument is turned off. Figure 5 shows the cooling curve of the soil sample.

The freezing temperature of free water at standard atmospheric pressure is 0 °C, while the pore water in the soil body makes its freezing temperature lower than 0°C due to its interaction with the surface of soil particles [27]. The freezing temperature of the soil is the temperature of pore water when it freezes stably. It is verified according to the fitting equation for freezing temperature of saline soils given by Chen [21].

$$-T_f = 2.8752\mathrm{W}^{-1.0509}\left(Cl^-\right)^{0.8427}\left(SO_4^{2-}\right)^{0.3575}. \quad (13)$$

Calculations based on the major negative ion content of the soil samples, brought into Equation 22, yielded a theoretical freezing temperature of -2.8°C for CS-2 and -23°C for CS-1. For CS-2 soil, the freezing temperature is -2.7°C, which is about 4% lower than the value predicted by the equation. However, the cooling curve of the CS-1 soil sample did not show any indication of freezing or latent heat release when the temperature reached -20°C, which indicates that the freezing temperature of CS-1 was at least -20°C lower, which is also consistent with the prediction of the equation. In fact, the field survey data of the road route showed that its salt content was generally greater than 10%, which implies that most saline soils along the route do not freeze in winter.

4.3. Strength Parameters. The relationship between the temperature measured by Zhang et al. [14] and the internal friction angle of cohesion according to the temperature interval is as follows:

The piece wise function relationship of HC-1 cohesion as a function of temperature and internal friction angle as a function of temperature is shown in equation (14):

$$C = \begin{cases} 58.2 - 1.86T & T \in (10, 20] \\ 50.1 - 1.05T & T \in (0, 10] \\ 50.1 - 0.81T & T \in (-10, 0] \\ 69 + 1.08T & T \in [-20, -10] \end{cases},$$

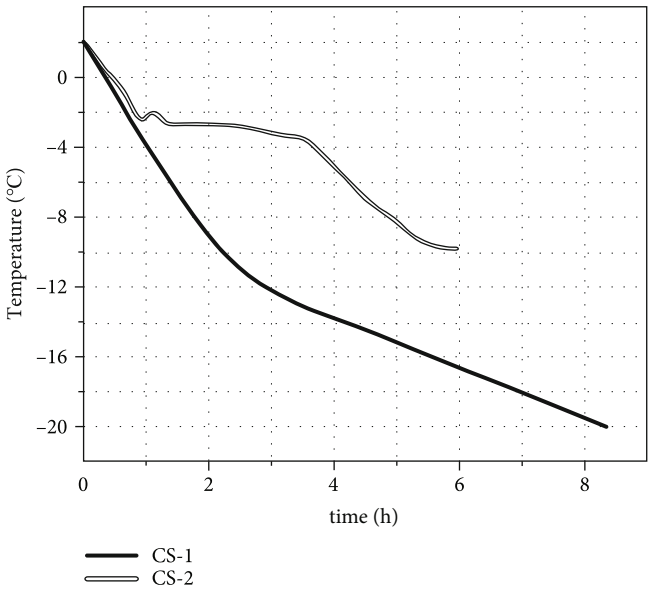

Figure 5: Cooling time history curve of the CS-1 and CS-2.

$$\varphi = \begin{cases} 37.1 - 0.03T & T \in (10, 20] \\ 36.9 - 0.01T & T \in (0, 10] \\ 36.9 - 0.02T & T \in (-10, 0] \\ 37.6 + 0.05T & T \in [-20, -10] \end{cases}. \quad (14)$$

The piece wise function relationship of HC-2 cohesion as a function of temperature and internal friction angle as a function of temperature is shown in equation (15):

$$C = \begin{cases} 57 - 1.38T & T \in (10, 20] \\ 50.4 - 0.72T & T \in (0, 10] \\ 50.4 - 1.28T & T \in (-10, 0] \\ 78.1 + 1.49T & T \in [-20, -10] \end{cases},$$

$$\varphi = \begin{cases} 34.1 - 0.02T & T \in (10, 20] \\ 33.9 & T \in (0, 10] \\ 33.9 - 0.04T & T \in (-10, 0] \\ 34.4 + 0.01T & T \in [-20, -10] \end{cases}. \quad (15)$$

The piecewise function relationship of CS-1 cohesion with temperature and internal friction angle with temperature (16) is shown as:

$$C = \begin{cases} 69.6 - 1.747T & T \in (10, 20] \\ 63 - 1.08T & T \in (0, 10] \\ 63 - 0.9T & T \in (-10, 0] \\ 71.4 - 0.06T & T \in [-20, -10] \end{cases},$$

$$\varphi = \begin{cases} 34.9 - 0.03T & T \in (10, 20] \\ 34.7 - 0.01T & T \in (0, 10] \\ 34.7 - 0.09T & T \in (-10, 0] \\ 34.6 - 0.1T & T \in [-20, -10] \end{cases}. \quad (16)$$

The piece wise function relationship of CS-2 cohesion with temperature and internal friction angle with temperature (17) is shown as:

$$C = \begin{cases} 90.6 - 1.32T & T \in (10, 20] \\ 84 - 0.66T & T \in (0, 10] \\ 84 - 2.16T & T \in (-10, 0] \\ 100.8 - 0.48T & T \in [-20, -10] \end{cases},$$

$$\varphi = \begin{cases} 38.3 - 0.06T & T \in (10, 20] \\ 37.8 - 0.01T & T \in (0, 10] \\ 37.8 - 0.13T & T \in (-10, 0] \\ 39 - 0.01T & T \in [-20, -10] \end{cases}. \quad (17)$$

Using Zhang et al. [12] to select natural foundation soil samples, direct shear experiments at different temperatures have obtained the relationship between the cohesion and internal friction angle of the foundation soil samples at different temperatures as shown in (18):

$$C = \begin{cases} 14 - 0.33T & T \in (10, 20] \\ 12.1 - 0.14T & T \in (0, 10] \\ 12.1 - 0.75T & T \in (-10, 0] \\ 27.7 + 0.81T & T \in [-20, -10] \end{cases},$$

$$\varphi = \begin{cases} 21.6 - 0.33T & T \in (10, 20] \\ 19.4 - 0.11T & T \in (0, 10] \\ 19.4 - 0.13T & T \in (-10, 0] \\ 21.3 + 0.06T & T \in [-20, -10] \end{cases}. \quad (18)$$

4.4. Values Based on Temperature Field Strength Parameters. When the temperature of the subgrade soil at a certain depth is determined, its strength parameter will be determined by the function of temperature and strength parameter. Applying the method above to theoretical calculations, as shown in Figure 6, it is assumed that the sliding surface is an arc sliding surface, i represents the ordinal number of soil strips, j represents the isotherm ordinal number passing through the bottom edge of the soil strip, C_{ij} represents the cohesion of the soil strip i when the j-th isotherm passes through the bottom edge of the soil strip i. Similarly, φ_{ij} is the magnitude of the internal friction angle of soil strip i when the j-th isotherm passes through the bottom edge of soil strip i. The

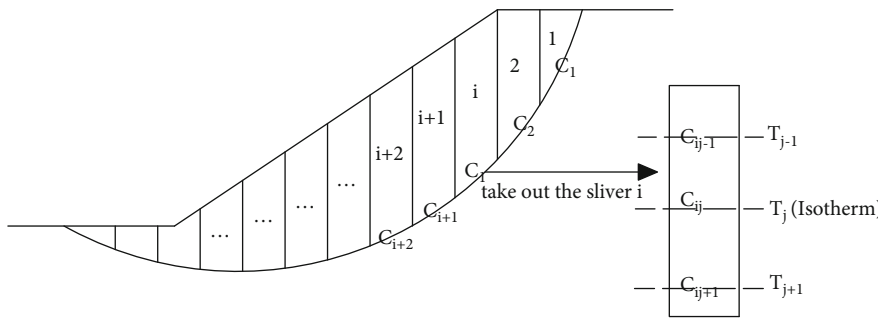

Figure 6: Determine cohesion based on isotherms.

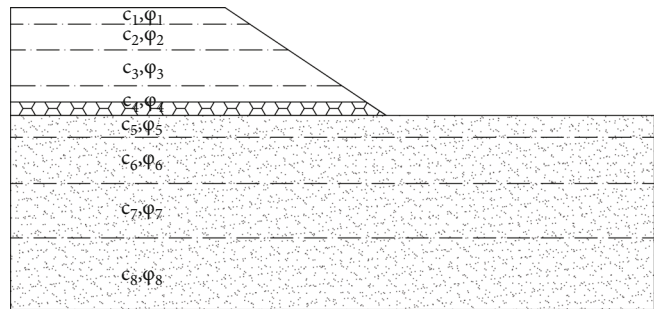

Figure 7: Schematic diagram of isothermal stratification-strength parameter model calculation.

value of C_{ij} and φ_{ij} can be determined by equations (14)~(18) by interpolation.

5. Calculation and Analysis of Slope Stability

5.1. Calculation of Safety Factor

5.1.1. Calculation Model of Isothermal Stratification—Strength Parameters. Combined with the function of the soil strength parameters and temperature measured in the laboratory, the isothermal layering-strength parameter calculation model is to layer the subgrade laterally in accordance with the soil isotherm of the subgrade, so as to calculating the safety factor of the subgrade slope and determining its slope stability. The value of strength to a certain depth is based on the temperature. The dashed line in Figure 7 indicates the isotherm. The strength parameters of each layer of soil were given according to the type of subgrade soil in the previous research. In the isothermal layering-strength parameter model, however, the subgrade is subdivided on the basis of previous achievements in accordance with the isotherm. It takes both the strength parameters of different soils and the changes in outside air temperature that affect the strength parameters of the soil into account. Obviously, the changes of soil strength parameters can be more accurate.

5.1.2. Solution Steps of SLOPE/W Module in GeoStudio

(1) Model rendering

(2) Material area generating. Divide the soil layer into different areas according to the isotherm and draw them separately. Number of isothermal lines = material area+1

(3) Material properties defining. Select the Mohr-Coulomb criterion and enter parameters such as cohesion, internal friction angle, bulk density, and elastic modulus

(4) Material area assignment. Add the material properties defined in step ③ to the corresponding material area defined in step ②

(5) Draw the water pressure line

(6) Draw the entrance and exit ranges of the sliding surface

(7) Model inspection. After the parameters of all models are defined, check whether the models are defined correctly and ensure that the subsequent calculations are performed normally

(8) Calculation and solution

The model calculation diagram is shown in Figure 8.

5.2. Stability Analysis of Subgrade Slope in Cold Season

5.2.1. Stability Analysis of Subgrade Slope under Heat

(1) Monthly Changes in Slope Stability. The subgrade fills are HC-1, HC-2, CS-1, and CS-2. When the subgrade width is 26 m, the subgrade height is 4 m, and the slope is 1: 1.5, the subgrade slope safety factor is shown in Figure 9.

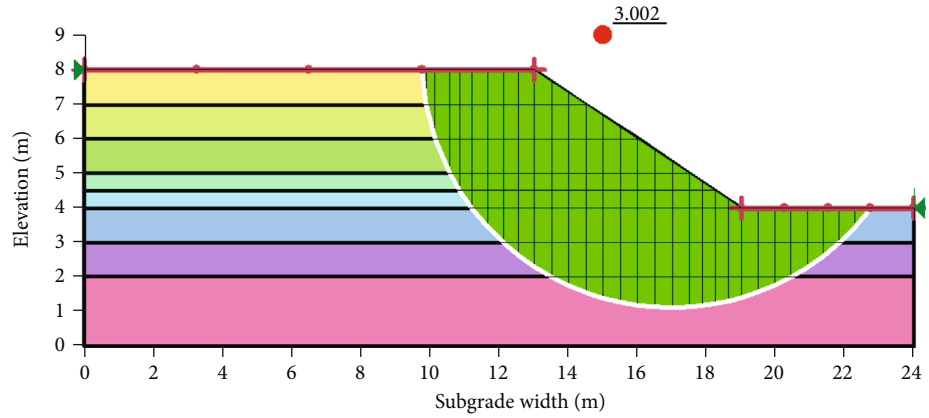

Figure 8: The calculation of the safety factor for January in the subgrade (4 m in height and 1 : 1.5 in slope) built on HC-1 soil.

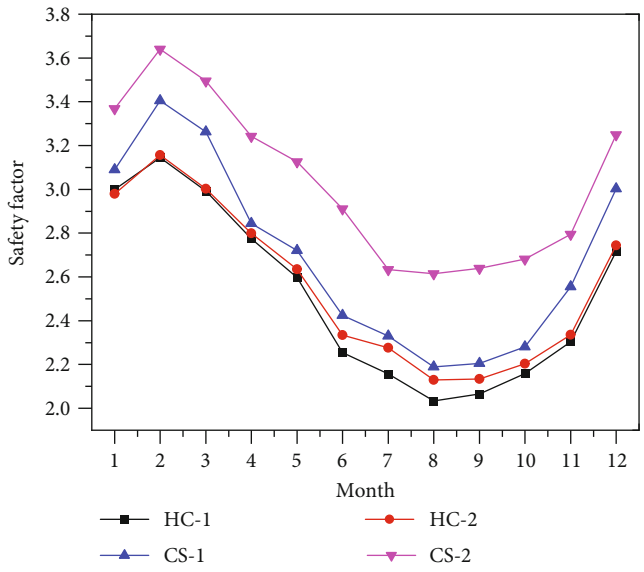

Figure 9: Monthly safety factor of subgrade slope.

(a) It can be seen from Figure 9 that, in general, the slope safety factors of the four groups of subgrades filled with soil samples change during these months, and its trend conforms to the variation law of sinusoidal function curve. In February, the slope safety coefficients reached their maximum values, and in August, it reached their minimum values, but the minimum values were greater than 2. In each month of the year, the subgrade slopes were stable

(b) In Figure 8, the safety coefficients of subgrade slopes in descending order throughout the year are CS-2, CS-1, HC-2, and HC-1. HC-1 soil-filled subgrade slope safety factor reached a maximum of about 3.1 in February and August reached a minimum value of about 2.0, which decreased by 35.5% in August compared with February; HC-2 soil-filled subgrade slope safety factor reached a maximum of about 3.2 in February, a minimum of about 2.1 in August, and a decrease of 34.4% in August compared with February; the safety factor of CS-1 soil subgrade slope reached a maximum of about 3.4 in February and a minimum of August. The value was about 2.2, which decreased by 35.3% in August compared with February; the safety factor of CS-2 soil-filled subgrade slope reached a maximum of about 3.6 in February, reached a minimum of about 2.6 in August, and decreased by 27.8 in August from February %. Among them, HC-1, HC-2, and CS-1 have similar declines, while CS-2 has a smaller decline

(c) Above all, the stability of the subgrade slope changes during the months in cold season. The stability in February is the best, and in August is relatively poor, but the minimum value of the safety factor is greater than 2. Comparing the information of air temperature and ground temperature, it can be concluded that the temperature below the surface reaches the minimum value in February, but reaches the maximum value in October. The temperature has a certain influence on the safety factor of the slope of saline soil subgrade, and the stability of the slope of saline soil subgrade is higher in the cold season than in the summer, but the slope of the subgrade is stable throughout the year, but the subgrade slope is stable throughout the year. Under the same construction conditions, the stability of subgrade slopes filled with saline soil with low chloride ion content is higher than that of saline soil with high chloride ion content

(2) Influence of Subgrade Height on Subgrade Slope Stability. Subgrade fillings are HC-1, HC-2, CS-1, and CS-2; the width of pavement is 26 m; slope of 1: 1.5; subgrade height is 3 m, 3.5 m, 4 m, 4.5 m, and 5 m, respectively; the safety factors of the subgrade slope in December, January, February, and March are shown in (a), (b), (c), and (d) in Figure 10.

(a) Subgrade filling HC-1
(b) Subgrade filling HC-2
(c) Subgrade filling CS-1
(d) Subgrade filling CS-2

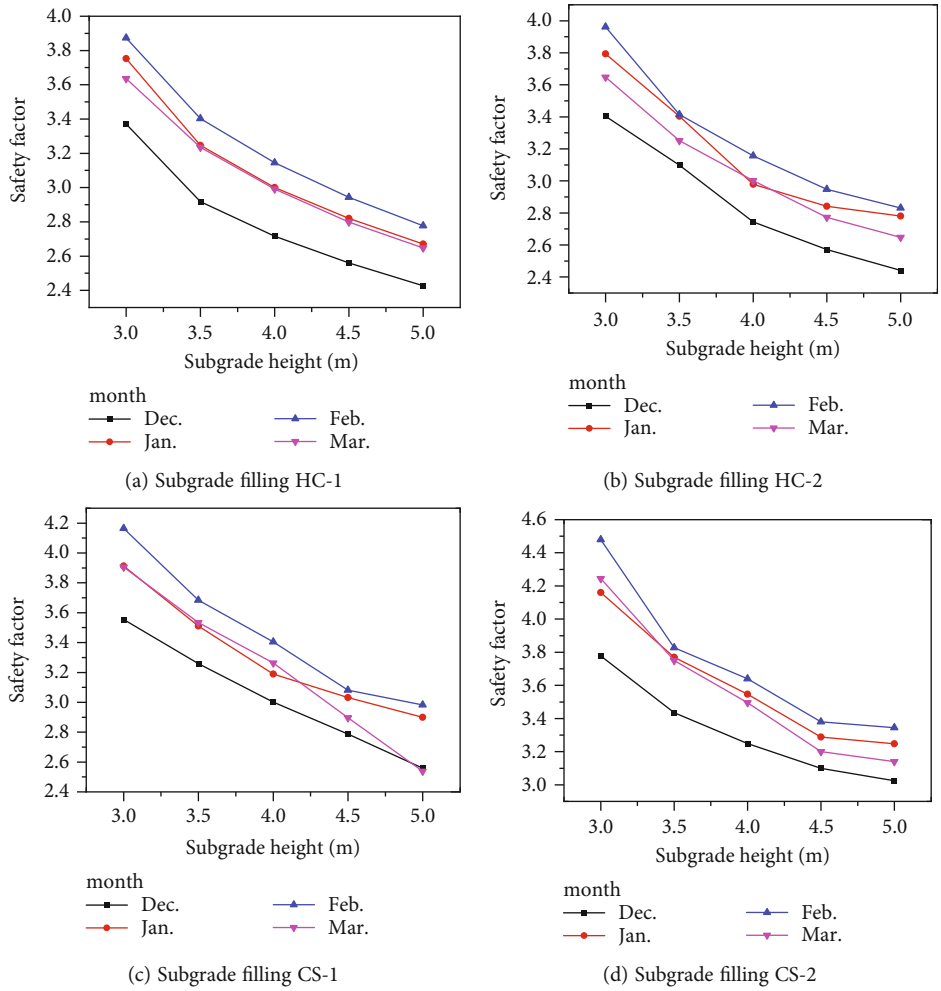

Figure 10: Different subgrade filling, slope 1 : 1.5, slope safety coefficient of different subgrade height in cold season.

(a) It can be seen from Figure 10 that in the cold season, when the height of the subgrade increases from 3 m to 3.5 m, 4 m, 4.5 m, and 5 m, the safety factor gradually decreases

(b) As can be seen from Figure 10(a), when the height of the HC-1 soil-filled subgrade increased from 3 m to 3.5 m, 4 m, 4.5 m, and 5 m, the safety factors in December were the lowest of the four months in the cold season, which dropped by 29.4% from about 3.4 to around 2.4; the safety factor in February was the highest of the four months in the cold season, which increased by 28.2% from about 3.9 to about 2.8

(c) As can be seen from Figure 10(b), when the height of the HC-2 soil-filled subgrade increased from 3 m to 3.5 m, 4 m, 4.5 m, and 5 m, the safety factor in December was the lowest of the four months in the cold season, which decrease by 29.4% from about 3.4 reduced to about 2.4; the safety factor in February was the highest of the four months in the cold season, which decrease by 30% from about 4.0 to about 2.8

(d) As can be seen from Figure 10(c), when the height of the CS-1 soil-filled subgrade increased from 3 m to 3.5 m, 4 m, 4.5 m, and 5 m, the safety factor in December was the lowest of the four months in the cold season; it was reduced from about 3.6 to about 2.6, a decrease of 27.8%; the safety factor in February was the highest in the four months of the cold season, from about 4.2 to about 3, a decrease of 28.6%.

(e) As can be seen from Figure 10(d), when the height of the subgrade filled with CS-2 soil is increased from 3 m to 3.5 m, 4 m, 4.5 m, and 5 m, the safety factor in December is the lowest of the four months in the cold season, from about 3.8 to about 3.0, a decrease of 21.1%; the safety factor in February was the highest of the four months in the cold season, from about 4.5 to about 3.3, a decrease of 26.7%.

(f) As the height of the subgrade increases (3~5 m), the safety factor decreases. In December, HC-1 and HC-2 soil-filled subgrade slopes experienced the fastest decline in safety factor, and in February, the HC-2 soil-filled subgrade slopes experienced the fastest decline in safety factor. The stability of the slope also

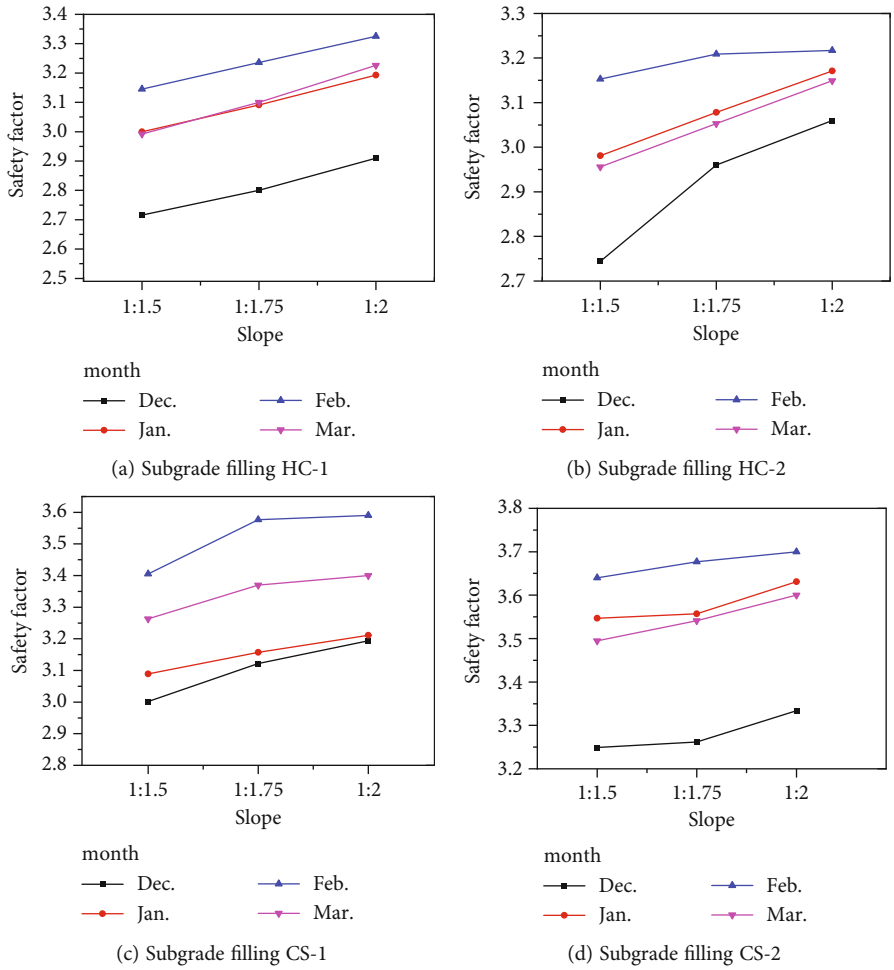

Figure 11: Different subgrade filling, slope safety factors with different gradients in the cold season.

decreases with the increase of the height of the subgrade, but the minimum value of all safety factors is greater than 2. When the height of the subgrade is 3~5 m, the slope is stable

(3) Influence of Subgrade Slope on Its Slope Stability. The subgrade fillings are HC-1, HC-2, CS-1, and CS-2, the width of the road surface is 26 m, and the height of the subgrade is 4 m. When the slopes are selected to be 1 : 1.5, 1 : 1.75, and 1 : 2, the safety factors of the subgrade slopes in December, January, and March are shown as (a), (b), (c), and (d) in Figure 11.

(a) Subgrade filling HC-1
(b) Subgrade filling HC-2
(c) Subgrade filling CS-1
(d) Subgrade filling CS-2

(a) As can be seen from Figure 11, in the cold season, if the slope reduced from 1 : 5 to 1 : 1.75 and 1 : 2, the slope safety factor generally increases

(b) As can be seen from Figure 11(a), if the slope of the subgrade filled with HC-1 soil decreased from 1 : 5 to 1 : 1.75 and 1 : 2, the slope safety factor in February is higher than the other months in the cold season, and the minimum value It is about 3.1, the maximum value is about 3.3, which is an increase of 6%; the slope safety factor in December is lower than other months in the cold season, the minimum value is about 2.7, the maximum value is about 2.9, and an increase of 7.4%

(c) As can be seen from Figure 11(b), when the slope of the subgrade filled with HC-2 soil reduced from 1 : 5 to 1 : 1.75 and 1 : 2, the slope safety factor in February was higher than that in other months in the cold season, and the minimum value is about 3.1, the maximum value is about 3.3, which increased by 6%; the slope safety factor in December is lower than other months in the cold season, the minimum value is about 2.7, the maximum value is about 3.1, and an increase of 14.8%

(d) As can be seen from Figure 11(c), when the slope of the subgrade filled with CS-1 soil slowed down from 1 : 5 to 1 : 1.75 and 1 : 2, the slope safety factor in February was higher than that in other months in

the cold season, and the minimum value is about 3.4, the maximum value is about 3.6, which increased by 5.9%; the slope safety factor in December is lower than other months in the cold season, with the minimum value of about 3.0, the maximum value of about 3.2, and an increase of 6.7%

(e) As can be seen from Figure 11(d), when the slope of the subgrade filled with CS-2 soil slowed down from 1 : 5 to 1 : 1.75 and 1 : 2, the slope safety factor in February was higher than that in other months in the cold season, and the minimum value is about 3.6, the maximum value is about 3.7, an increase of 2.8%; the slope safety factor in December is lower than other months in the cold season, the minimum value is about 3.2, the maximum value is about 3.3, and an increase of 3.1%

(f) As the slope of the subgrade slows down (1 : 1.5 to 1 : 2), the safety factor increases. The fastest increase in the safety factor in February was the subgrade slopes filled with HC-1 and HC-2 soil, and the fastest increase in the safety factor in December was in the subgrade slopes filled with HC-2 soil. The stability of the slope also increases as the slope of the subgrade slows down. All safety factors are greater than 2.7. When the slope of the subgrade is 1 : 1.5~1 : 2, its slope is stable

(g) Measures to improve the stability of subgrade slopes. During the construction process, the salt content of the saline soil subgrade fill is strictly controlled; insulate the slope of the subgrade to reduce the amplitude of the change of temperature gradient and prevent the influence of large temperature difference on the stability of the slope of the subgrade; geotextiles or geomembranes are placed between the different layers of the roadbed slope to block the migration of water and salts and prevent the accumulation of salts that can lead to the reduction of the stability of the subgrade slope

6. Conclusion

The author used COMSOL simulation to simulate the temperature field of the subgrade in Qarham area. With that, an isothermal layering-strength parameter model is proposed. The author used the SLOPE/W module in GeoStudio to calculate the safety factor of the subgrade slope in the cold region. The main conclusions are:

(1) The numerical simulation results are consistent with the numerical change trend of the measured data of boreholes, and the validity of the temperature field simulation is verified

(2) As the temperature changes, the strength of the subgrade soil changes accordingly. Based on the establishment of isothermal layering-strength parameter model, the analysis towards stability process of the subgrade slope in the cold region is done

(3) The monthly variation curve of the safety factor of the subgrade slope is very close to the sinusoidal function curve. With the season changes, the safety factor also changes; the stability gradually decreases with the increase of the subgrade height in the cold season, of which HC-2 fill of subgrades fell the most in February, about 30%. As the slope of the subgrade reduced (1 : 1.5, 1 : 1.75, 1 : 2), the stability gradually increased. The subgrade filled with HC-2 had the largest increase in February, about 14.8%.

Data Availability

The [DATA TYPE] data used to support the findings of this study are included within the article.

Conflicts of Interest

The authors declare that they have no conflicts of interest.

Acknowledgments

This research was jointly supported by grants from the National Natural Science Foundation of China (No. 41501062) and the Longyuan Youth Innovation and Entrepreneurship Talent (Team) Project of Gansu Province. This support is much appreciated.

References

[1] X. S. Wang, H. Zhang, and M. Xue, "Road diseases and prevention in saline soil areas," *Journal of Tongji University (Natural Science Edition)*, vol. 10, pp. 1178–1182, 2003.

[2] J. McRobert and G. Foley, *The Impacts of Waterlogging and Salinity on Road Assets: A Western Australian Case Study*, 1999.

[3] D. A. Swenne, *The Eutectic Crystallization of nacl·2h$_2$o and ice, [Ph.D. thesis]*, Technische Hogeschool Eindhoven, 1983.

[4] M. Liao, Y. Lai, and C. Wang, "A strength criterion for frozen sodium sulfate saline soil," *Canadian Geotechnical Journal*, vol. 53, no. 7, pp. 1176–1185, 2016.

[5] D. G. Archer, "Thermodynamic properties of the NaCl+H_2O system. II. Thermodynamic properties of NaCl(aq), NaCl·2H_2(cr), and phase equilibria," *Journal of Physical & Chemical Reference Data*, vol. 21, no. 4, pp. 793–829, 2009.

[6] H. Bing and W. Ma, "Experimental Study on Freezing Point of Saline Soil," *Journal of Glaciology & Geocryology*, vol. 33, no. 5, pp. 1106–1113, 2011.

[7] A. Banin and D. M. Anderson, "Effects of salt concentration changes during freezing on the unfrozen water content of porous materials," *Water Resources Research*, vol. 10, no. 1, pp. 124–128, 1974.

[8] A. G. Weeks, "The stability of natural slopes in south-east England as affected by periglacial activity," *Quarterly Journal of Engineering Geology & Hydrogeology*, vol. 2, no. 1, pp. 49–61, 1969.

[9] J. N. Hutchinson, "Periglacial solifluxion: an approximate mechanism for clayey soils," *Géotechnique*, vol. 24, no. 3, pp. 438–443, 1974.

[10] E. C. Mcroberts and N. R. Morgenstern, "The stability of thawing slopes," *Canadian Geotechnical Journal*, vol. 11, no. 4, pp. 447–469, 1974.

[11] G. Rongali, A. K. Keshari, A. K. Gosain, and R. Khosa, "Split-window algorithm for retrieval of land surface temperature using Landsat 8 thermal infrared data," *Journal of Geovisualization & Spatial Analysis*, vol. 2, no. 2, p. 8, 2018.

[12] J. H. Fang, M. Huo, and J. Z. Zhang, *Technology for Highway Engineering in Permafrost and Saline Soil Regions*, Lanzhou University Press, Lanzhou, 2011.

[13] L. L. Cai, R. H. Gao, and J. Y. Liu, "Engineering geological zoning and subgrade salt blocking technology in Salt Lake area of Chage expressway," *Subgrade Engineering*, vol. 14, pp. 1–5, 2015.

[14] Y. Zhang, J. Fang, J. Liu, and A. Xu, "Research on the distribution of saline soil along the Chaerhan-Golmud Highway," *Sciences in Cold and Arid Regions*, vol. 7, no. 2, pp. 0189–0193, 2015.

[15] Y. Zhang, Z. H. Yang, J. K. Liu, and J. H. Fang, "Impact of cooling on shear strength of high salinity soils," *Cold Regions Science and Technology*, vol. 141, pp. 122–130, 2017.

[16] Q. B. Bai, X. Li, and Y. H. Tian, "Study on coupled equations and numerical simulations of water and heat in frozen soil," *Chinese Journal of Geotechnical Engineering*, vol. 37, no. 2, pp. 131–136, 2015.

[17] Q. Xia, S. Dou, and C. J. Zhao, "Experimental study on moisture migration and frost heave during the freezing process of the Lanxin railway subgrade," *China Railway Science*, vol. 33, no. 5, pp. 1–7, 2012.

[18] G. S. Taylor and J. N. Luthin, "A model for coupled heat and moisture transfer during soil freezing," *Canadian Geotechnical Journal*, vol. 15, no. 4, pp. 548–555, 1978.

[19] Y. H. Tian, J. K. Liu, Z. Y. Qian et al., "Numerical simulation of temperature field of subgrade with insulation layer in permafrost region," *China Railway Science*, vol. 23, no. 2, pp. 59–64, 2002.

[20] N. Lu and L. I. K. O. S. William, *Mechanics of Unsaturated Soils*, vol. 23, Higher Education Press, Beijing, 2012.

[21] X. B. Chen, J. K. Liu, H. X. Liu et al., *Soil Freezing and Foundation*, Science Press, Beijing, 2006.

[22] Y. B. Cao, Y. Sheng, J. C. Wu et al., "Influence of upper boundary conditions on simulated ground temperature field in permafrost regions," *Journal of Glaciology and Geocryology*, vol. 36, no. 4, pp. 802–810, 2014.

[23] J. C. Wang and S. D. Li, "Analysis of thermal conditions near the lower limit surface of permafrost along the Qinghai-Tibet Highway," *Proceedings of Qinghai-Tibet Frozen Soil*, , pp. 38–43, Science Press, Beijing, 1983.

[24] Q. B. Wu, G. L. Jiang, Y. B. Pu, and Y. S. Deng, "Relationship between permafrost and gas hydrates on Qinghal-Tibet Plateau," *Geological Bulletin of China*, vol. 25, no. 1, pp. 29–33, 2006.

[25] J. E. T. Houghton, Y. H. Ding, J. Griggs et al., *Climate Change*, The Scientific Basis, BeiJing, 2001.

[26] D. H. Qin, Y. H. Ding, and S. W. Wang, "A study of environment change and its impacts in western China," *Earth Science Frontiers*, vol. 9, no. 2, pp. 321–328, 2002.

[27] X. Z. Xu, J. C. Wang, and L. X. Zhang, *Frozen Soil Physics*, Science Press, Beijing, 2001.